

**UNCLASSIFIED**

---

---

**AD 403 433**

*Reproduced  
by the*

**DEFENSE DOCUMENTATION CENTER**

FOR

**SCIENTIFIC AND TECHNICAL INFORMATION**

**CAMERON STATION, ALEXANDRIA, VIRGINIA**



---

---

**UNCLASSIFIED**

NOTICE: When government or other drawings, specifications or other data are used for any purpose other than in connection with a definitely related government procurement operation, the U. S. Government thereby incurs no responsibility, nor any obligation whatsoever; and the fact that the Government may have formulated, furnished, or in any way supplied the said drawings, specifications, or other data is not to be regarded by implication or otherwise as in any manner licensing the holder or any other person or corporation, or conveying any rights or permission to manufacture, use or sell any patented invention that may in any way be related thereto.

CATALOGED BY ASTIA  
AS AD 10 403433

E-1210

**SIMPLIFIED ANALYSIS OF FLEXIBLE  
BOOSTER FLIGHT CONTROL SYSTEMS**

by

**Lee Gregor Hofmann and Allen Kezer**

June 1962

15 BDC  
1962

**INSTRUMENTATION  
LABORATORY**

This document has been classified as  
public release in that it, at, for  
Security Review, OSD, on **AUG 15 1962**

**MASSACHUSETTS INSTITUTE OF TECHNOLOGY**

Cambridge 39. Mass.

E-1210

**SIMPLIFIED ANALYSIS OF FLEXIBLE  
BOOSTER FLIGHT CONTROL SYSTEMS**

by

Lee Gregor Hofmann and Allen Kezer

June 1962

**INSTRUMENTATION LABORATORY  
MASSACHUSETTS INSTITUTE OF TECHNOLOGY**

*Prepared for publication by Jackson & Moreland, Inc.*

Approved:   
Deputy Associate Director

Approved:   
Associate Director

---

## ACKNOWLEDGMENT

The research program leading to this paper was carried out under the auspices of the Massachusetts Institute of Technology DSR Project 52-156, sponsored by the Ballistic Systems Division of the Air Research and Development Command through USAF Contract AF 04(647)-303.

## ABSTRACT

Structural flexibility effects exert a considerable influence upon the stability of booster orientation flight control systems. This paper presents a relatively simple method of using root locus techniques to develop the factored open loop relating function for the system including these flexibility effects. The analysis procedure is very useful in the design of these control systems since the solution to the stability problems encountered becomes evident from the form of the factored open loop relating function.

The particular manner in which the development takes place enables one to understand the effects of the major design and physical parameters upon the form of the open loop relating function, and in so doing, bridges the gap between these parameters and their effect on the performance of the closed loop system.

Armed with the basic understanding which the analysis procedure provides, it is possible to interpret the performance of a parameter adjusting adaptive control system or to formulate rapidly the preliminary design of a fixed parameter flight control system.

TABLE OF CONTENTS

	<u>Page</u>
INTRODUCTION. . . . .	1
ANALYSIS OF THE OPEN LOOP PERFORMANCE FUNCTION OF THE FLIGHT CONTROL SYSTEM . . . . .	2
Functional Description of Control System . . . . .	3
Mathematical Description of System Dynamics . . . . .	3
Example Illustrating the Method of Applying the Simplified Analysis . . . . .	14
RELATION OF CONTROL SYSTEM ANALYSIS TO CONTROL SYSTEM DESIGN . . . . .	26
SUMMARY . . . . .	29
 <u>Appendix</u>	
A    APPROXIMATE LINEARIZED EQUATIONS OF MOTION IN A SINGLE PLANE FOR A FLEXIBLE BOOSTER. . . . .	31
B    OBTAINING THE FLEXIBLE BOOSTER RELATING FUNCTION WHICH INCLUDES COMPENSATION. . . . .	37
REFERENCES . . . . .	43

# **SIMPLIFIED ANALYSIS OF FLEXIBLE BOOSTER FLIGHT CONTROL SYSTEMS**

by

**Lee Gregor Hofmann and Allen Kezer**

## **INTRODUCTION**

Structural flexibility effects have been extremely important in the design of flight control systems for large ballistic missiles and boosters. As the size of the vehicles has increased, the lightly damped structural modes of vibration have moved into the same frequency range that is desired for the flight control system so that strong coupling effects have resulted. The nature of these coupling effects has been such that it has been difficult to achieve adequate stability margins for all flight conditions. The relatively low stability margins have necessitated complex and detailed analysis of the systems to insure that the margins do indeed exist and that uncertainties in the knowledge of vehicle parameters will not lead to system instabilities.

In the process of the development of an adaptive control system to overcome some of these obstacles, it was necessary to develop simplified analysis techniques which would lead to a better understanding of the effects of parameters upon the performance of the system. These simplified analysis techniques are useful not only in the design of adaptive control systems but also in the preliminary design of a basic control system to which the adaptive features may be added if necessary.

One of the prime considerations in the design of the flight control systems is the fact that the sensors which provide the means of closing the feedback loops (gyros, accelerometers, etc.) sense the local bending at the sensor station as well as the motion of the ideal rigid body. In some cases, a very

significant improvement can be made in the closed loop bending dynamics by use of proper feedback of the bending information that is sensed by these instruments. This can result in a very significant reduction in the bending motion and hence in the dynamic loads which are applied to the structure.

In any feedback control system, the feedback signal must have the proper phase and amplitude. Usual root locus or frequency response methods of analysis which are used to insure the existence of the proper phase and amplitude require that the open loop poles and zeros of the system transfer function be known in factored form. This paper employs a relatively simple and systematic method of obtaining the factored open loop transfer function for a booster control system using simplified equations of motion and a root locus factorization technique.

The development illustrates the application of this technique to the case of a system which controls the orientation of the undeflected centerline of the booster. In this system the feedback quantities are angular displacement and rate of angular displacement with respect to inertial space of the flexed centerline of the booster at one or more locations along the centerline.

The feedback of other quantities, such as normal acceleration, may be included in the control system by developing an applicable set of equations using the method of derivation employed in this paper. The simplifying assumptions which make this systematic analysis possible do not cause any significant loss in accuracy in the description of the physical booster, and because of the dynamic similarity of the booster modes of motion, the analysis is effective in reducing the apparent complexity of the problem. The effects of the important booster characteristics and design parameters upon system performance are quite evident, and parametric studies are greatly facilitated by this particular method of obtaining the open loop relating function.

#### ANALYSIS OF THE OPEN LOOP PERFORMANCE FUNCTION OF THE FLIGHT CONTROL SYSTEM

In order to analyze the effects of parameter variations on the closed loop performance of the booster flight control system, the open loop relating function must be known in factored form. To proceed toward this end, a mathematical description of the control system must be formulated from a functional description of the system.

### Functional Description of Control System

A functional block diagram of an orientation flight control system is presented in Fig. 1. This system utilizes feedback of angular orientation information as sensed by rate and rate integrating gyros. In many cases, the orientation measurement may be performed by the inertial measurement unit of the guidance system instead of a separate rate integrating gyro. Angular orientation or angular rate may be commanded to the system by suitable usage of the orientation measuring instrument. The input and output variables of the system are different for the different commands, but the loop dynamics and analysis procedures are unaffected.

The rate and rate integrating gyros may be located at different stations along the booster body. If necessary, the outputs of several rate (or rate integrating) gyros may be summed in such a way that the rigid body component is the same as that sensed by a single gyro, while the effective bending mode slope "sensed" for each mode may be changed by suitable adjustment of the contribution made by each gyro.

The introduction of compensation into the control loops provides several additional system variables which in turn make it possible to use different approaches for stabilizing the different modes considered in the design. For generality, compensation units are placed at three locations in the two control loops of Fig. 1.

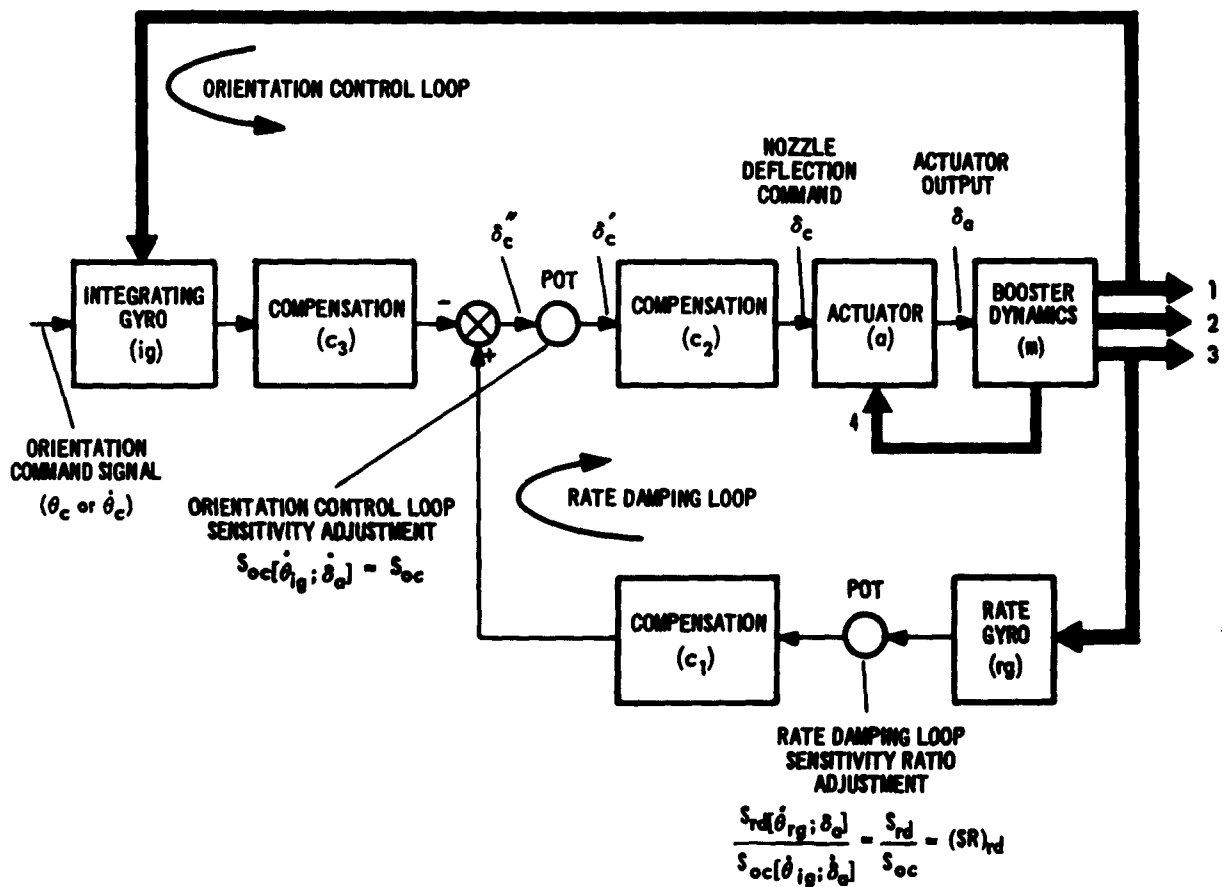
In this study, it is assumed that a gimballed nozzle is used for the thrust vector control and that a hydraulic actuator is used to provide the required nozzle deflection. For clarity, a first order lag approximation is used for the hydraulic actuator and a second order system for the nozzle dynamics. Accelerations of the nozzle gimbal point which produce reaction torques on the nozzle and couple the rigid body and bending modes with the nozzle motion are neglected, but may be included by mathematical operations which are similar to those developed in this paper.

### Mathematical Description of System Dynamics

The equations of motion which have been developed for the booster airframe are quite complex\* and use of these complete equations is cumbersome. To facilitate analysis and interpretation of parametric effects, the equations may be simplified without any significant loss in accuracy. In Appendix A,

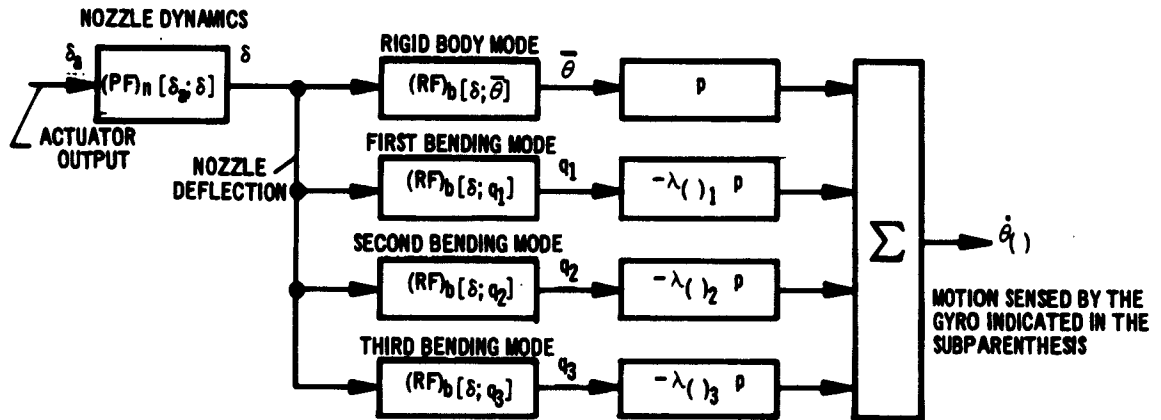
---

\* See Appendix A



- 1 MOTION WITH RESPECT TO INERTIAL SPACE SENSED BY THE INTEGRATING GYRO ( $\dot{\theta}_{ig}$ )
- 2 MOTION OF BOOSTER UNDEFLECTED CENTER LINE WITH RESPECT TO INERTIAL SPACE ( $\theta$ )
- 3 MOTION WITH RESPECT TO INERTIAL SPACE SENSED BY THE RATE GYRO ( $\dot{\theta}_{rg}$ )
- 4 INERTIAL LOADING EFFECT UPON ACTUATOR

Fig. 1. Functional block diagram of booster flight control system.



THE EQUATIONS FOR THE ABOVE RELATING FUNCTIONS ARE LISTED BELOW

**BOOSTER RELATING FUNCTIONS**

$$(PF)_n [\delta_a; \delta] = \frac{1}{\left(1 + \frac{2\zeta_n}{\omega_n} p + \frac{p^2}{\omega_n^2}\right)}$$

$$S_b [\delta; \ddot{\theta}] = \frac{S_b [\delta; \ddot{\theta}] I}{\omega_{z_0}^2} \quad \omega_{z_0}^2 = -\frac{S_b [\delta; \ddot{\theta}] I}{I_E}$$

$$(RF)_b [\delta; \ddot{\theta}] = \frac{S_b [\delta; \ddot{\theta}] \left(1 + \frac{p^2}{\omega_{z_0}^2}\right)}{p^2}$$

$$\omega_{z_1}^2 = \frac{T_{\phi_{g_i}} \left(1 - \frac{I_E}{I}\right) - \frac{T}{m} \lambda_{g_i} m_n l_{ni}}{m_n l_i} \approx \frac{T_{\phi_{g_i}}}{m_n l_i}$$

$$(RF)_b [\delta; q_i] = \frac{S_b [\delta; q_i] \left(1 + \frac{p^2}{\omega_{z_1}^2}\right)}{\left(1 + \frac{2\zeta_i}{\bar{\omega}_i} p + \frac{p^2}{\bar{\omega}_i^2}\right)}, \quad i=1, 2, 3$$

$$l_i = l_n \phi_{g_i} - \frac{I_n}{m_n} \lambda_{g_i}$$

$$I_E = I_n + m_n l_n l_g$$

$$S_b [\delta; \ddot{\theta}] = -\frac{T l_g}{I} \left(1 + \frac{m_n l_n}{n l_g}\right) \approx -\frac{T l_g}{I}$$

$$\bar{\omega}_i = 1 - \frac{T_{\phi_{g_i}} \lambda_{g_i}}{m \omega_i^2} \approx 1$$

$$S_b [\delta; q_i] = -\left[ \frac{T_{\phi_{g_i}} \left(1 - \frac{I_E}{I}\right) - \frac{T}{m} \lambda_{g_i} m_n l_n}{m \omega_i^2 \bar{\omega}_i} \right] \approx -\frac{T_{\phi_{g_i}}}{m \omega_i^2}$$

Fig. 2. Block diagram representation of the simplified booster dynamics.  
(The effects of three bending modes are included.)

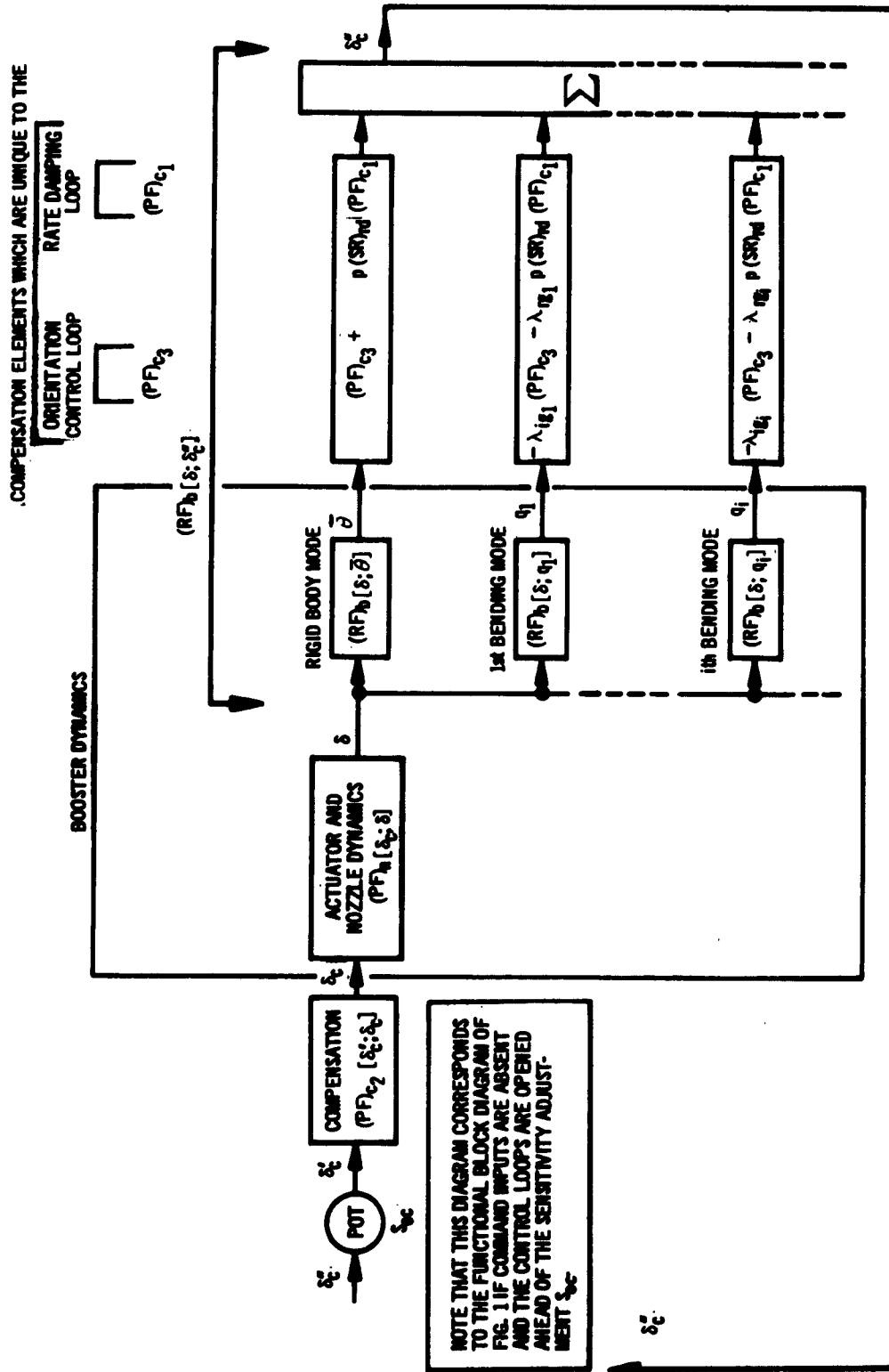


Fig. 3. Mathematical block diagram of the open loop booster control system for an arbitrary number of bending modes - simplified equations of motion.

the complete linearized equations have been simplified to a degree which permits the relating function for the  $\dot{\theta}_{rg}$  output of the Booster Dynamics functional block of Fig. 1 to be represented by the block diagram of Fig. 2 when the (rg) notation is substituted in the subparenthesis of  $\theta_{( )}$  and  $\lambda_{( )}_i$ . The relating function for the  $\dot{\theta}_{ig}$  output may be represented by the same block diagram using the (ig) notation. This diagram in Fig. 2 is a general representation of the booster equations from a nozzle deflection ( $\delta$ ) to the motion sensed by a single gyro ( $\theta_{( )}$ ).

The relating function paths of the rate damping and orientation control loops can be combined into one path for each booster mode. The mathematical block diagram of the resulting open loop relating function is shown in Fig. 3. The opening in the control loops depicted in Fig. 3 corresponds to an opening ahead of the sensitivity adjustment,  $S_{oc}$ , in the forward portion of the control loops of Fig. 1.

The parallel paths shown in Figs. 2 and 3 result from the fact that the gyros sense a component of angular motion due to the local slope of each bending mode as well as the angular motion of the rigid body. The factor which represents the local slope of each bending mode ( $\lambda_{( )}_i$ ) appears as a separate sensitivity factor in the mathematical block diagrams<sup>i</sup> of Figs. 2 and 3. The slope of the  $i^{\text{th}}$  bending mode at the integrating gyro station is denoted by  $\lambda_{ig_i}$  and at the rate gyro station by  $\lambda_{rg_i}$ . In Fig. 3 the parallel paths also contain the compensation elements which are unique to either the rate damping loop or the orientation control loop.

The open loop performance function of the booster control system may be written by inspection of Fig. 3:

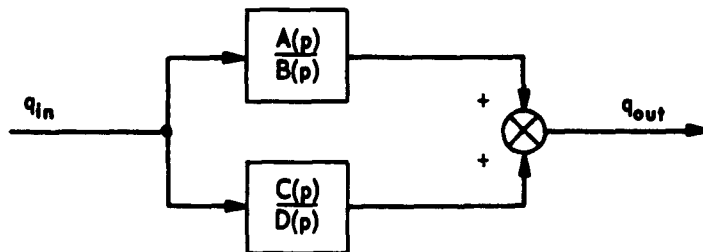
$$(\text{PF})_{\text{bcs}}^{\text{open loop}} = (\text{RF})_{\text{b}}[\delta; \delta_c''] S_{oc} (\text{PF})_{c_2}[\delta_c'; \delta_c] (\text{PF})_{\text{n}}[\delta_c; \delta]$$

The parallel paths of the open loop relating function which compose  $(\text{RF})_{\text{b}}[\delta; \delta_c'']$  and represent the components of the control system feedback signal due to nozzle deflection, must be reduced to a single path. Algebraic reduction of the expressions for these parallel paths to an expression for a single path results in a ratio of polynomials with a factored denominator and

an unfactored numerator. The numerator polynomial must be factored before proceeding with an analysis of the closed loop control system.

The development of the expressions for obtaining the factors of the numerator polynomial is based on the algebraic manipulation of the sum of two polynomials into a familiar unity feedback expression to which root locus factoring techniques may be applied.

For example:



A, B, C, D,  $q_{in}$ , and  $q_{out}$  are functions of  $p$ ; A, B, C, and D are factored polynomials in  $p$ .

$$\begin{aligned} \frac{q_{out}}{q_{in}} &= \frac{A}{B} + \frac{C}{D} = \frac{AD + CB}{BD} \\ &= \frac{1}{BD} \left\{ AD \left[ 1 + \frac{BC}{AD} \right] \right\} \\ &= \frac{1}{BD} \left\{ \left[ \frac{BC}{AD} \right] \frac{1}{BC} \right\}^{-1} \end{aligned}$$

If A, B, C, and D are factored polynomials, the quantity of the inner brackets [ ] may be factored by a root locus where the "open loop" poles are the factors of A and D and the "open loop" zeros are the factors of B and C. Because of the minus unity exponent on the term in the outer bracket { }, the locus of the poles of the root locus factorization becomes a locus of the numerator zeros of the  $q_{out}/q_{in}$  transfer function.

The determination of the zeros of the relating function of the open loop booster control system shown in Fig. 3 involves the successive application of this technique as the parallel path for each bending mode is added to the analysis. The equations for the determination of the zeros are presented in Equation Summary 1 for the case in which the compensation units  $c_1$  and  $c_3$  have transfer functions of unity.\* The expressions for including one bending mode in parallel with the rigid body mode are given by equations 1-3(a), (b), (c), and 1-4.

The extension of this result to allow the addition of the effects of a bending mode when an arbitrary number of bending modes have already been included in parallel with the rigid body mode is given by Eqs. 1-7(a), (b), (c), and 1-8.

---

\*The results of a similar development for a more general case in which the compensation units  $c_1$  and  $c_2$  do not have performance functions of unity is presented in Appendix B. However, the results there are mainly of academic interest, since the effects of these compensation unit dynamics may be accurately represented by simpler means. The simpler method involves defining and calculating effective values of the local bending mode slopes "sensed" by the rate and integrating gyros. These effective values of the slopes are equivalent, in the system performance sense, to the combination of the actual values of the local bending mode slopes sensed by the gyros and the effects of the compensation.

Assuming that the performance functions of the  $c_1$  and  $c_3$  compensation units are equal to unity, the following expression for  $(RF)_b[\delta; \delta_c^*]$  can be developed from the mathematical block diagram of Fig. 3 and the relating functions listed in Fig. 2

$$(RF)_b[\delta; \delta_c^*] = \frac{S_b[\delta; \ddot{\theta}] \left(1 + \frac{p^2}{\omega_{z_0}^2}\right)}{p^2} \left(1 + p (SR)_{rd}\right) + \frac{\lambda_{1g1} S_b[\delta; q_1] \left(1 + \frac{p^2}{\omega_{z_1}^2}\right)}{\left(1 + \frac{2\zeta_1}{\bar{\sigma}_1 \omega_1} p + \frac{p^2}{\bar{\sigma}_1 \omega_1^2}\right)} \left(1 + p (SR)_{rd} \frac{\lambda_{rg1}}{\lambda_{1g1}}\right) \quad (1-1)$$

The first term in the above expression is the contribution of the rigid body motion to the  $\delta_c^*$  signal; the second term is the contribution of the 1st mode motion. Placing the above expression over a common denominator gives

$$= \frac{S_b[\delta; \ddot{\theta}]}{p^2 \left(1 + \frac{2\zeta_1}{\bar{\sigma}_1 \omega_1} p + \frac{p^2}{\bar{\sigma}_1 \omega_1^2}\right)} \left[ \left(1 + \frac{2\zeta_1}{\bar{\sigma}_1 \omega_1} p + \frac{p^2}{\bar{\sigma}_1 \omega_1^2}\right) \left(1 + \frac{p^2}{\omega_{z_0}^2}\right) \left(1 + (SR)_{rd} p\right) + -p^2 \frac{\lambda_{1g1} S_b[\delta; q_1]}{S_b[\delta; \ddot{\theta}]} \left(1 + \frac{p^2}{\omega_{z_1}^2}\right) \left(1 + (SR)_{rd} \frac{\lambda_{rg1}}{\lambda_{1g1}} p\right) \right] \quad (1-2)$$

Introducing a simplifying notation

$$= \frac{S_b[\delta; \ddot{\theta}]}{p^2 \left(1 + \frac{2\zeta_1}{\bar{\sigma}_1 \omega_1} p + \frac{p^2}{\bar{\sigma}_1 \omega_1^2}\right)} [A_1(p) + K_1 B_1(p)] \quad (1-3)$$

where

$$A_1 = \left(1 + \frac{2\zeta_1}{\bar{\sigma}_1 \omega_1} p + \frac{p^2}{\bar{\sigma}_1 \omega_1^2}\right) \left(1 + \frac{p^2}{\omega_{z_0}^2}\right) (1 + (SR)_{rd} p) \quad (1-3a)$$

Equation Summary 1 (Page 1 of 4)  
Development of the Flexible Booster Relating Function -  
Without Compensation  $[(PF)_{c_1} = (PF)_{c_3} = 1]$

$$B_1 = p^2 \left( 1 + \frac{p^2}{\omega_{z1}^2} \right) \left( 1 + (SR)_{rd} \frac{\lambda_{rg1}}{\lambda_{ig1}} p \right) \quad (1-3b)$$

$$K_1 = \frac{-\lambda_{ig1} S_b[\delta; q_1]}{S_b[\delta; \bar{\theta}]} \quad (1-3c)$$

In Eqs. (1-2) and (1-3) the five zeros of the relating function are contained in the bracketed term. One zero results from the rate gyro "differentiation"; two from placing the polynomials over a common denominator, and two "tail-wags-dog" zeros from the inertial reactions of the gimballed nozzle. Care must be taken not to confuse the "tail-wags-dog" zero of the booster which is a factor of  $(RF)_b[\delta; \delta_c^*]$  with the "tail-wags-dog" zero of the *i*th mode which is a factor of  $(RF)_b[\delta; q_1]$ .

By rearranging the bracketed term of Eq. (1-3), the polynomial summation  $A_1 + K_1 B_1$ , may be put into the familiar unity feedback form, multiplied by a factored polynomial,  $1/K_1 B_1$ .

$$(RF)_b[\delta; \delta_c^*] = \frac{S_b[\delta; \bar{\theta}]}{p^2 \left( 1 + \frac{2\zeta_1}{\bar{a}_1 \omega_1} p + \frac{p^2}{\bar{a}_1 \omega_1^2} \right)} \left\{ \left[ \frac{K_1 \frac{B_1}{A_1}}{1 + K_1 \frac{B_1}{A_1}} \right] \frac{1}{K_1 B_1} \right\}^{-1} \quad (1-4)$$

The quantity in the inner brackets of Eq. (1-4) is the unity feedback expression which is readily factored by root locus techniques.

The final factored form of the relating function is obtained by completing the other algebraic operations that are indicated in Eq. (1-4); noting especially the minus unity exponent of the outer bracketed term.

The effects of additional bending modes can be included in the relating function by similar operations.

In adding the second mode the equations become

$$(RF)_b[\delta; \delta_c^*] \Big|_{\substack{\text{for first} \\ \text{and second} \\ \text{modes}}} = (RF)_b[\delta; \delta_c^*] \Big|_{\substack{\text{for first} \\ \text{mode}}} - \frac{\lambda_{ig2} S_b[\delta; q_2] \left( 1 + \frac{p^2}{\omega_{z2}^2} \right)}{\left( 1 + \frac{2\zeta_1}{\bar{a}_2 \omega_2} p + \frac{p^2}{\bar{a}_2 \omega_2^2} \right)} \left( 1 + p (SR)_{rd} \frac{\lambda_{rg2}}{\lambda_{ig2}} \right) \quad (1-5a)$$

Equation Summary 1 (Page 2 of 4)  
 Development of the Flexible Booster Relating Function -  
 Without Compensation  $[(PF)_{c1} = (PF)_{c3} = 1]$

Examination of the above equation suggests that it is possible to generalize it immediately to the case where the nth mode is being added to the expression for the (n-1) mode relating function. Additionally, it can be seen that it is not necessarily the mode n which must be added at this point since any of the other (n-1) modes might have been used in its place. Therefore, the mode added will be denoted j to indicate that the modes need not be included in order according to their mode index.

The method for the calculation of the relating function which includes n bending modes when the relating function which includes (n-1) modes is known, is derived in the following operations.

$$(RF)_{b[\delta; \delta_c^*]} \Big|_{\text{for } n \text{ modes}} = (RF)_{b[\delta; \delta_c^*]} \Big|_{\text{for } (n-1) \text{ modes}} - \frac{\lambda_{1g_j} S_b[\delta; q_j] \left(1 + \frac{p^2}{\omega_{z_j}^2}\right)}{\left(1 + \frac{2\zeta_j}{\bar{a}_j \omega_j} p + \frac{p^2}{\bar{a}_j \omega_j^2}\right)} \left(1 + p (SR)_{rd} \frac{\lambda_{rg_j}}{\lambda_{1g_j}}\right) \quad (1-5b)$$

The first term in the above expression is the contribution of the rigid body motion and (n-1) of the n bending modes to the  $\delta_c^*$  signal; the second term is the contribution of the jth mode motion.

Substituting the factored form of  $(RF)_{b[\delta; \delta_c^*]} \Big|_{\text{for } (n-1) \text{ modes}}$  and placing the above expression over a common denominator gives

$$\begin{aligned} (RF)_{b[\delta; \delta_c^*]} \Big|_{\text{for } n \text{ modes}} &= \frac{S_b[\delta; \theta]}{p^2 \prod_1^n \left(1 + \frac{2\zeta_i}{\bar{a}_i \omega_i} p + \frac{p^2}{\bar{a}_i \omega_i^2}\right)} \times \\ &\times \left[ \left( \begin{array}{l} \text{the } (2n+1) \text{ zeros of} \\ (RF)_{b[\delta; \delta_c^*]} \text{ for } (n-1) \text{ modes} \end{array} \right) \left(1 + \frac{2\zeta_j}{\bar{a}_j \omega_j} p + \frac{p^2}{\bar{a}_j \omega_j^2}\right) + \right. \\ &\quad \left. - \frac{\lambda_{1g_j} S_b[\delta; q_j]}{S_b[\delta; \theta]} p^2 \left(1 + \frac{p^2}{\omega_{z_j}^2}\right) \left(1 + (SR)_{rd} \frac{\lambda_{rg_j}}{\lambda_{1g_j}} p\right) \right] \times \\ &\times \prod_1^{n-1} \left(1 + \frac{2\zeta_i}{\bar{a}_i \omega_i} p + \frac{p^2}{\bar{a}_i \omega_i^2}\right) \end{aligned} \quad (1-6)$$

Equation Summary 1 (Page 3 of 4)  
Development of the Flexible Booster Relating Function -  
Without Compensation  $[(PF)_{e_1} = (PF)_{e_3} = 1]$

Introducing simplifying notation

$$(RF)_b[\delta; \delta_c^n] \Big|_{\text{for } n \text{ modes}} = \frac{S_b[\delta; \bar{\theta}]}{p^2 \prod_i^n \left(1 + \frac{2\zeta_i}{\bar{\omega}_i} p + \frac{p^2}{\bar{\omega}_i^2}\right)} [A_j(p) + K_j B_j(p)] \quad (1-7)$$

where

$$A_j(p) = \left(1 + \frac{2\zeta_j}{\bar{\omega}_j} p + \frac{p^2}{\bar{\omega}_j^2}\right) \times$$

$$\times [\text{the } (2n+1) \text{ zeros of } (RF)_b[\delta; \delta_c^n] \text{ for } (n-1) \text{ modes}] \quad (1-7a)$$

$$B_j(p) = p^2 \left(1 + \frac{p^2}{\omega_{zj}^2}\right) \left(1 + (SR)_{rd} \frac{\lambda_{rgj}}{\lambda_{igj}} p\right)^{n-1} \left(1 + \frac{2\zeta_i}{\bar{\omega}_i} p + \frac{p^2}{\bar{\omega}_i^2}\right) \quad (1-7b)$$

$$K_j = \frac{-\lambda_{igj} S_b[\delta; q_j]}{S_b[\delta; \bar{\theta}]} \quad (1-7c)$$

The  $2n+1$  zeros of Eqs. (1-6) and (1-7a) must be expressed in the form  $\left(1 + \frac{2\zeta}{\omega} p + \frac{p^2}{\omega^2}\right)$  or  $(1 + \tau p)$ .  
Rearranging Eq. (1-7) into the familiar unity feedback form gives

$$(RF)_b[\delta; \delta_c^n] \Big|_{\text{for } n \text{ modes}} = \frac{S_b[\delta; \bar{\theta}]}{p^2 \prod_i^n \left(1 + \frac{2\zeta_i}{\bar{\omega}_i} p + \frac{p^2}{\bar{\omega}_i^2}\right)} \left[ \frac{K_j \frac{B_j}{A_j}}{1 + K_j \frac{B_j}{A_j}} \right] \frac{1}{K_j B_j} \Bigg]^{-1} \quad (1-8)$$

The order of the polynomials  $A_j(p)$  and  $B_j(p)$  is  $(2n+3)$  for  $n=2, 3, 4, \dots$ . The explanation of the origin of the zeros is the same as before, but in addition, two zeros appear for each bending mode added.

Equation Summary 1 (Page 4 of 4)  
Development of the Flexible Booster Relating Function –  
Without Compensation  $[(PF)_{c_1} = (PF)_{c_2} = 1]$

### Example Illustrating the Method of Applying the Simplified Analysis

The usefulness of this simplified analysis in qualitative applications cannot be fully appreciated until one witnesses a demonstration of its power and simplicity in an actual example. It is the experience of the authors and our associates that the routine of formal operations indicated in equations 1-4 and 1-8 of Equation Summary 1 are easily carried out to obtain the factors of the numerator polynomial of  $(RF)_{b[\delta; \delta_c'']}$ ; to wit:

**Problem:** Find the factors of the numerator polynomial of  $(RF)_{b[\delta; \delta_c'']}$  for a case in which the first and second bending mode effects are included in the analysis.

**Situation:** 1. The orientation and rate damping control loops contain the same compensation which is lumped into the  $c_2$  element of Fig. 1. The  $c_1$  and  $c_3$  compensation transfer functions are therefore equal to unity.

2. The damping of the bending modes is assumed to be negligible.

$$\zeta_1 = \zeta_2 \cong 0$$

3. The "tail-wags-dog" frequencies,  $\omega_{z_0}$ ,  $\omega_{z_1}$ ,  $\omega_{z_2}$  of the rigid body, first bending, and second bending mode, respectively, are related by the following inequality. \*

$$\omega_{z_0} > \omega_{z_1} > \omega_{z_2}$$

4. The first and second bending mode frequencies are such that

$$\omega_1 \sqrt{a_1} < \omega_{z_2} \quad **$$

---

\* It can be shown that the "tail-wags-dog" frequencies are almost invariably related to one another by the above inequality. The greatest of these frequencies is slightly less than  $\sqrt{\frac{T}{m_n l_n}}$ . Differences between the frequencies in the inequality are small.

An interesting fact is that the "tail-wags-dog" frequencies are relatively constant during a constant thrust flight profile as opposed to the bending mode frequencies which may increase over 100% during the flight profile.

\*\* Note that  $\omega_1 \sqrt{a_1}$  is the undamped natural frequency of the  $i^{\text{th}}$  bending mode when the rocket engine is thrusting; this is also the resonant frequency when the damping of the  $i^{\text{th}}$  mode is negligible.

and

$$\omega_2 \sqrt{g_2} > \omega_{z_0}$$

The first bending mode resonant frequency is less than the lowest "tail-wags-dog" frequency, and the second bending mode frequency is greater than the highest "tail-wags-dog" frequency.

5. The sign of the ratio of the bending mode slope sensed by the gyros at their respective stations to the bending mode displacement at the nozzle gimbal station is given for each mode by:

a)  $\lambda_{ig1}/\phi_{g1}$ ,  $\lambda_{rg1}/\phi_{g1}$  and  $\lambda_{ig2}/\phi_{g2}$  are negative

b)  $\lambda_{rg2}/\phi_{g2}$  is positive

c)  $\lambda_{ig1}/\phi_{g1} = \lambda_{rg1}/\phi_{g1}$

**Qualitative Solution:**

The zeros of  $(RF)_{b[\delta, \delta_c]}$  including the first bending mode in parallel with the rigid body mode are determined by one root locus operation. The effects of the second bending mode in parallel with the combination of the rigid body and first bending mode are added by a second root locus operation. The steps of the qualitative solution of the problem are outlined below. These correspond to the mathematical operations indicated in Eqs. 1-4 and 1-8 of Equation Summary 1. Figures 4 (a-d) are graphical representations of these steps.

1. Since  $(PF)_{c_1} = (PF)_{c_3} = 1$ , the equations of Equation Summary 1 are applicable to this problem. The first bending mode will be added first. Plot the open loop roots of the term in the inner brackets of Eq. 1-4,  $B_1(p) / A_1(p)$  on the complex plane. The poles are the roots from Eq. 1-3(a) and the zeros are the roots from Eq. 1-3(b). Since  $\lambda_{ig1} / \phi_{g1} = \lambda_{rg1} / \phi_{g1}$ ,  $A_1(p)$  and  $B_1(p)$  contain common factors of  $[1+p(SR)_{rd}]$  which divide out.

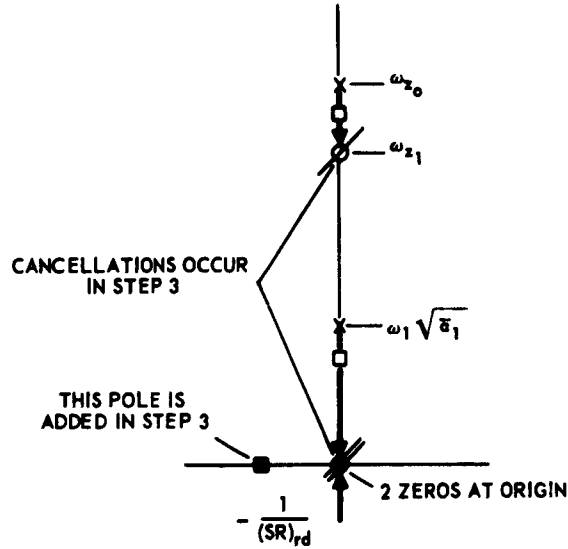


Fig. 4(a). Root locus determination of the flexible booster relating function – steps 1 through 3.

RESULT IS  $(RF)_b[\delta; \delta'_c]$  INCLUDING THE FIRST BENDING MODE ONLY

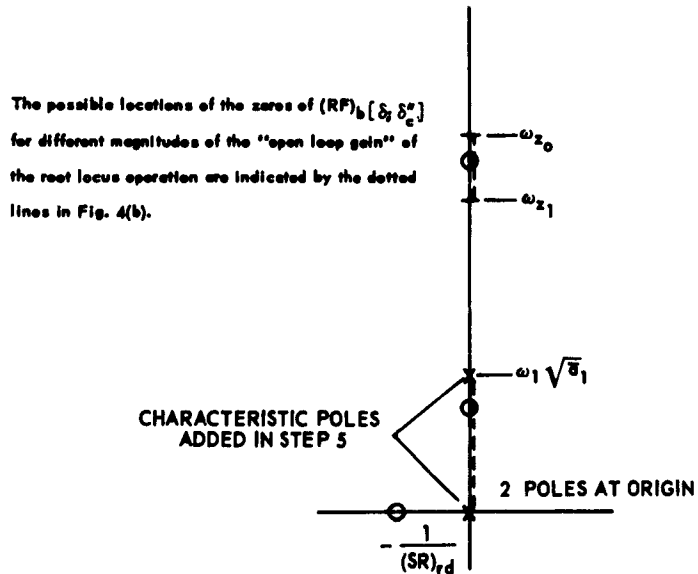


Fig. 4(b). Root locus determination of the flexible booster relating function – steps 4 and 5.

2. Find the roots of  $\left\{ K_1 (B_1 / A_1) / [1 + K_1 (B_1 / A_1)] \right\}$  by the root locus technique. Care must be taken to choose the proper angle criterion for the locus. The locus criterion for this part of the problem is  $180^\circ$ . The root locus is easily sketched by inspection since all of the open loop roots lie on the imaginary axis in the "p" plane. Note that increasing the magnitude of  $\lambda_{rg_1} = \lambda_{ig_1}$  corresponds to increasing the magnitude of the open loop gain and therefore causes the closed loop poles to move away from the open loop poles along the imaginary axis toward the zeros.
3. After finding the roots of  $\left\{ K_1 (B_1 / A_1) / [1 + K_1 (B_1 / A_1)] \right\}$ , multiply through by the remaining term in the outer brackets,  $1 / K_1 B_1$ . Cancellations with all open loop zeros occur, and the sensitivity of the outer bracketed term becomes unity.
4. Invert the bracketed function. The minus unity exponent on the brackets corresponds to changing the poles remaining after step 3 to zeros. These zeros are the zeros or factors of the numerator of the relating function  $(RF)_{b[\delta; \delta_c]}$  including the first bending mode.
5. Multiply the function resulting from step 4 by the sensitivity and characteristic poles outside of the outer bracketed function (add these characteristic poles to the root locus plot). The resulting plot is now  $(RF)_{b[\delta; \delta_c]}$  including the first bending mode.

To add the effects of the second mode, apply the operations of Eq. 1-8 for  $n=j=2$ .

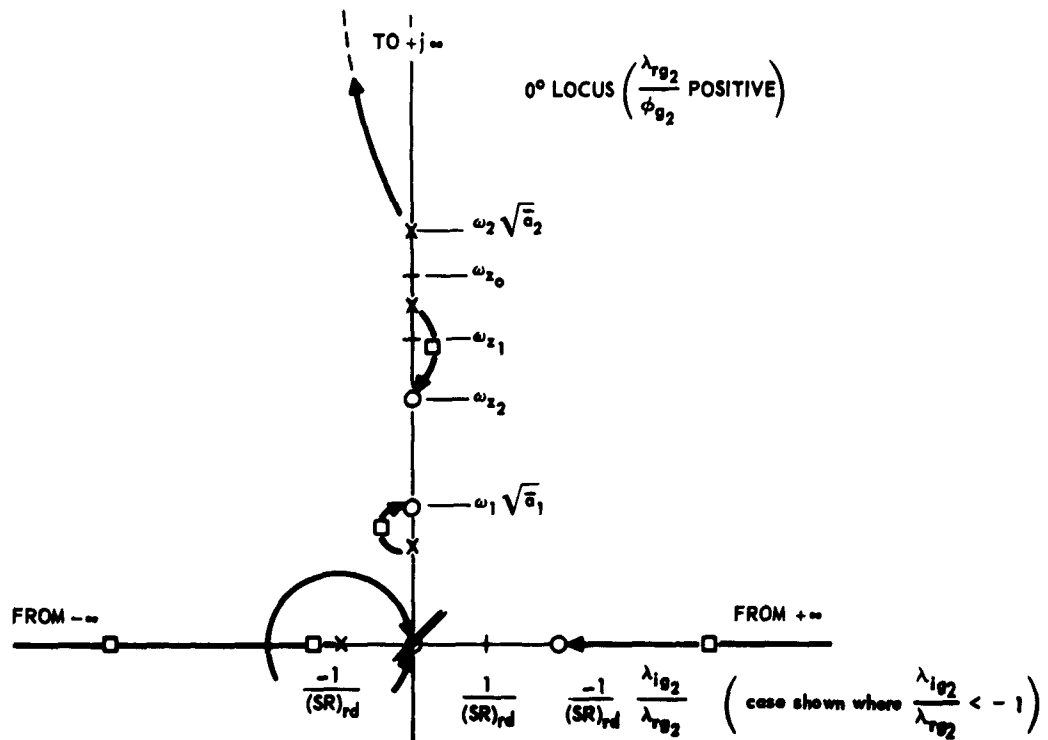


Fig. 4(c). Root locus determination of the flexible booster relating function - steps 6 thru 8.

RESULT IS  $(RF)_b[\delta; \delta_c^*]$  INCLUDING THE FIRST AND SECOND BENDING MODES.

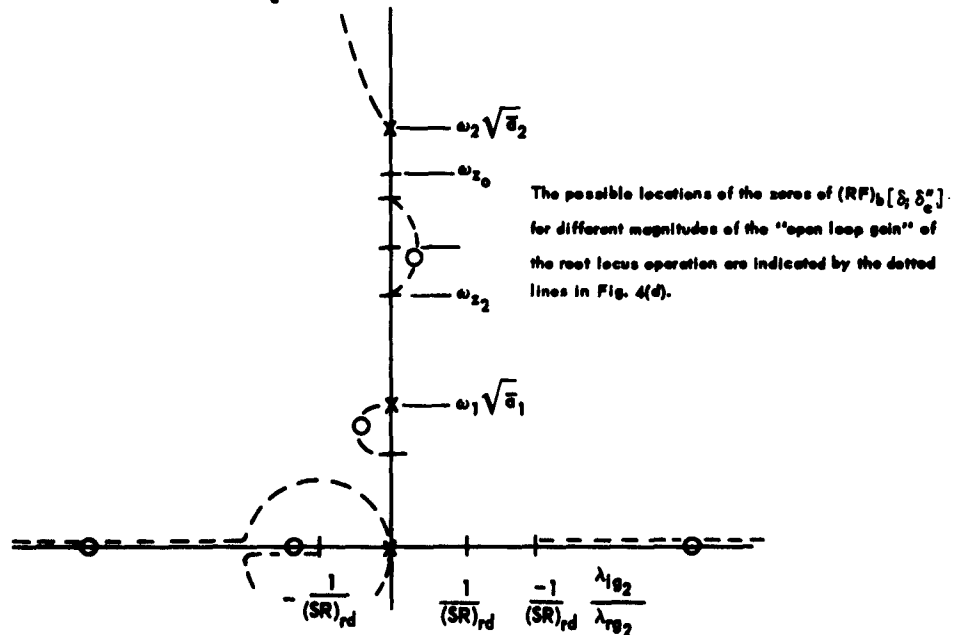


Fig. 4(d). Root locus determination of the flexible booster relating function - steps 9 and 10.

6. Proceed as in step 1 this time plotting  $B_2/A_2$  as the open loop roots of the term in the inner brackets. Note in Eq. 1-7(a) that the roots of  $A_2$  are the  $2n+1(n=2)$  poles remaining after the operations of step 3 plus the two roots which are the characteristic of the bending mode being added (second bending mode). In Eq. 1-7(b),  $B_2$  has roots as follows: 2 at the origin, 2 at the "tail-wags-dog" frequency of the bending mode being added,  $2n-2(n=2)$  corresponding to the characteristic roots of the bending modes already included, and one from the effect of different rate gyro and rate integrating gyro pickups of the second bending mode slope component of angular deflection. Since  $\lambda_{ig_2} \neq \lambda_{rg_2}$ ,  $[1 + p(SR)_{rd} \lambda_{rg_2} / \lambda_{ig_2}]$  of  $B_2$  and  $[1 + p(SR)_{rd}]$  of  $A_2$  do not divide out as did the corresponding factors for the first bending mode. Steps 7 through 10 are similar to steps 2 through 5. In step 10, however, an additional pair of characteristic poles appear outside of the outer bracketed term. These are the characteristic poles of the second bending mode. The resulting plot is now  $(RF)_{b[\delta; \delta_c'']}$  including the effects of the first and second bending modes.

Following are several important observations to note as a consequence of this example; some are directly obvious, the others result from a bit of qualitative experimentation with the parameters of the system.

1. The open loop singularities used in a locus operation are either the singularities of the relating functions for the booster modes listed in Fig. 2, or the roots of the numerator polynomial of  $(RF)_{b[\delta; \delta_c'']}$  which were found as a result of the previous locus operation.

2. The form of the root locus operation is such that the zeros due to the inclusion of the  $i^{\text{th}}$  bending mode proceed from the open loop pole locations of the  $i^{\text{th}}$  bending mode with increasing magnitude of the  $i^{\text{th}}$  mode slope sensed by the rate gyro,  $\lambda_{rg_i}$ . The parameter  $\lambda_{rg_i}$  is a design variable because its value is determined by the placement of the rate gyro along the booster body.
3. The direction in which the zeros due to the inclusion of the  $i^{\text{th}}$  mode proceed from the  $i^{\text{th}}$  mode pole locations is determined by the sign of  $\lambda_{rg_i}$ , the relative value of the  $i^{\text{th}}$  bending mode resonant frequency to the  $i^{\text{th}}$  mode "tail-wags-dog" frequency,\* and the value of  $\lambda_{ig_i} / \lambda_{rg_i}$ .\*\* The parameter  $\lambda_{ig_i}$  is a design variable because its value is determined by the placement of the rate integrating gyro along the booster body.
4. If  $\lambda_{rg_i} = \lambda_{ig_i} = \lambda_{G_i}$  for all the modes included in the analysis, one zero of  $(RF)_{b[\delta; \delta_c]}$  occurs on the real axis at  $-1/(SR)_{rd}$ . The rest of the zeros occur in conjugate imaginary pairs, in real pairs symmetric about the origin, or in complex conjugate foursomes which are symmetric about the imaginary axis.
5. If  $\lambda_{rg_i} = \lambda_{ig_i} = \lambda_{G_i}$  for all the modes included in the analysis, the phase of  $(RF)_{b[\delta; \delta_c]} / [1 + p(SR)_{rd}]$  at each resonant frequency can be easily calculated knowing only the parameters of the modes and the mode slope sensed by the gyros,  $\lambda_{G_i}$ . In a similar fashion the phase or range of phase at each of the zeros is easily calculated even though the positions of the zeros are only quantitatively known.

---

\*i. e.  $\omega_i \sqrt{a_i}$  less than or greater than  $\omega_{z_i}$ .

\*\*Other parameters assumed constant.

The assumption that  $\lambda_{rg_i} = \lambda_{ig_i} = \lambda_{G_i}$  is often useful to make even if the statement is not strictly true because of the substantial "computational" simplification which is introduced. This assumption does not effect the position of the zeros relative to the poles in the direction of the imaginary coordinate. The parameter ratio  $\lambda_{ig_i} / \lambda_{rg_i}$  controls the lateral location, or real coordinate of the zeros with respect to the poles. This control is usually rather weak except when  $1 / (SR)_{rd}$  tends to zero and/or  $|\lambda_{ig_i} / \lambda_{rg_i}|$  tends to be large with respect to unity. When the control of  $\lambda_{ig_i} / \lambda_{rg_i}$  is weak, its effect does not alter the basic nature of the problem, and therefore the assumption is useful when only qualitative understanding of a problem is required.

The statement  $\lambda_{rg_i} = \lambda_{ig_i}$  is strictly true when both rate and rate integrating gyros are placed at the same station along the booster body.

A figure which emphasizes points 4 and 5 above, follows. This will show the zero-pole configurations that  $(RF)_{b[\delta; \delta_c]}$  may assume for all possible combinations of  $\lambda_{G_i} / \phi_{g_i}$  greater or less than zero and  $\omega_i \sqrt{a_i} / \omega_{z_i}$  greater or less than unity\* when one bending mode is included in the analysis. Four

---

\*If the mode slope parameters  $\lambda_{rg_i}$  and  $\lambda_{ig_i}$  or  $\lambda_{G_i}$  are divided by the  $i^{th}$  mode displacement at the gimbal station  $\phi_{g_i}$ , the resulting ratios are independent of the manner in which the mode shapes are normalized. It can be shown that the sign of this ratio indicates the phase of the  $i^{th}$  mode component of motion sensed by the gyro relative to the phase of the force being applied to the  $i^{th}$  mode.

The expression  $\omega_i \sqrt{a_i}$  greater or less than  $\omega_{z_i}$  can be non-dimensionalized by dividing through by  $\omega_{z_i}$  to produce a neater mathematical statement. This ratio indicates the dominance of the transverse component of thrust acting on the  $i^{th}$  mode over the transverse component of the inertial reaction force due to gimbaling the nozzle at the resonant frequency of the  $i^{th}$  mode when  $(\omega_i \sqrt{a_i} / \omega_{z_i}) < 1$ . When  $(\omega_i \sqrt{a_i} / \omega_{z_i}) > 1$  this ratio indicates that the transverse inertial reaction force is dominant over the transverse component of thrust acting on the  $i^{th}$  mode at the resonant frequency of the  $i^{th}$  mode. Note that the transverse inertial reaction force on the  $i^{th}$  mode is  $180^\circ$  out of phase with the transverse component of the thrust acting on the  $i^{th}$  mode when the nozzle is gimballed at an arbitrary frequency.

basic combinations are possible; these are shown in Fig. 5(a-d). Alternate features which can arise in cases 3 and 4 of Figs. 5(a-d) are shown in Figs. 5(e-g). The method by which these figures were constructed exactly parallels steps 1 through 5 of the previous example which showed the method for obtaining the zeros of  $(RF)_{b[\delta; \delta_c'']}$ .

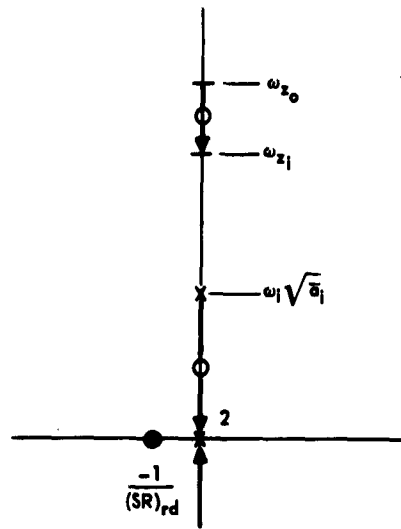
Table 1 shows the phase or range of phase at each singularity of  $(RF)_{b[\delta; \delta_c'']} / [1+p(SR)_{rd}]$  for the different cases based on observations of Fig. 5(a-g).

The areas of the complex plane in which the zeros are found for the different cases are compiled in Table 2. This table is also based on observations of Fig. 5(a-g).

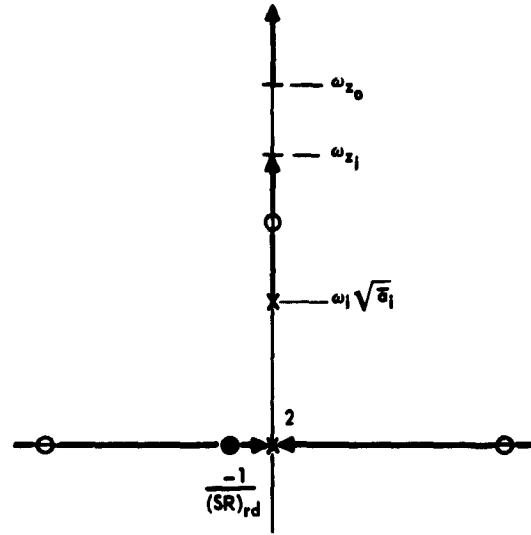
The significance of tables such as 1 and 2 greatly increases when they are constructed for cases which include more than one bending mode in the analysis. When several modes are considered, it will be apparent to the control system designer that this classification procedure is helpful in keeping track of such things as the possible pole-zero configurations and phase-at-the-singularities of  $(RF)_{b[\delta; \delta_c'']}$ .

When all possible combinations of the relative values of  $\lambda_{G_i} / \phi_{g_i}$  to zero and of  $\omega_i \sqrt{a_i} / \omega_{z_i}$  to unity for all the modes included in an analysis are qualitatively investigated, patterns of zero locations relative to the poles are evident. These patterns, which are uniquely specified in terms of the relative values of these parameters, can be translated into tables similar to 1 and 2. Subsequent use of the tables requires knowledge of  $\lambda_{G_i} / \phi_{g_i}$  and  $\omega_i \sqrt{a_i} / \omega_{z_i}$  for the modes of the particular booster of interest, but does not require even a qualitative factorization of  $(RF)_{b[\delta; \delta_c'']}$  since its approximate pole-zero configuration can be reconstituted from the tables once they have been constructed.

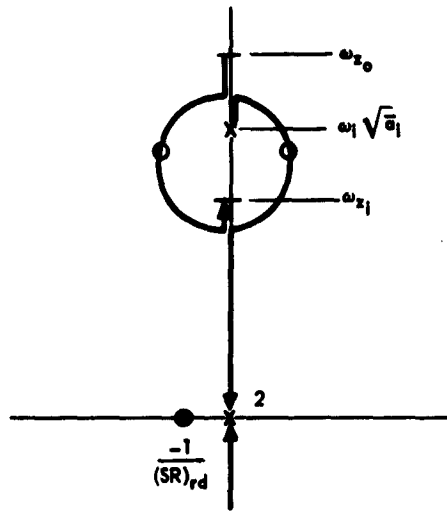
In the next section it is shown how particular patterns of pole-zero relationships of the booster relating function directly influence the choice of the  $c_2$  compensation unit for the control system and the closed loop performance of the booster flight control system. Hence reference to these tables aids in making a quick identification of those areas in which the design of a particular booster flight



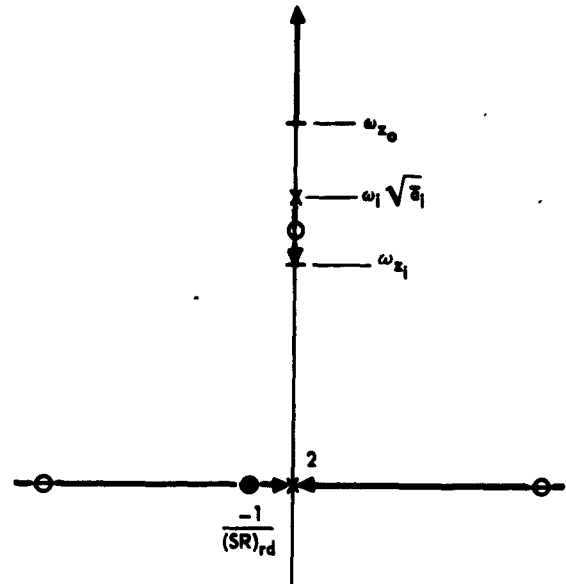
a. Case 1 ( $\lambda_{G_1}/\phi_{g_1} < 0, \omega_1 \sqrt{\alpha_1}/\omega_{z_1} < 1$ )



b. Case 2 ( $\lambda_{G_1}/\phi_{g_1} > 0, \omega_1 \sqrt{\alpha_1}/\omega_{z_1} < 1$ )

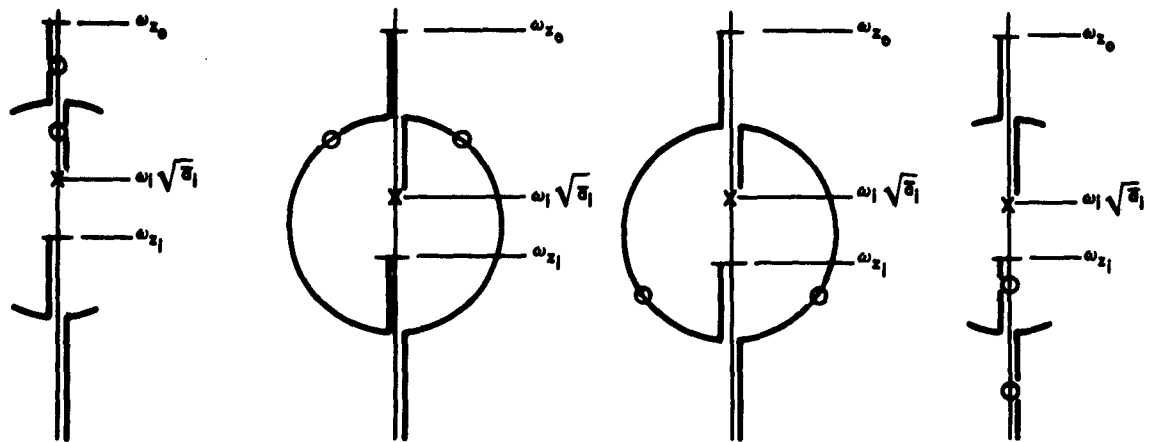


c. Case 3 ( $\lambda_{G_1}/\phi_{g_1} < 0, \omega_1 \sqrt{\alpha_1}/\omega_{z_1} > 1$ )



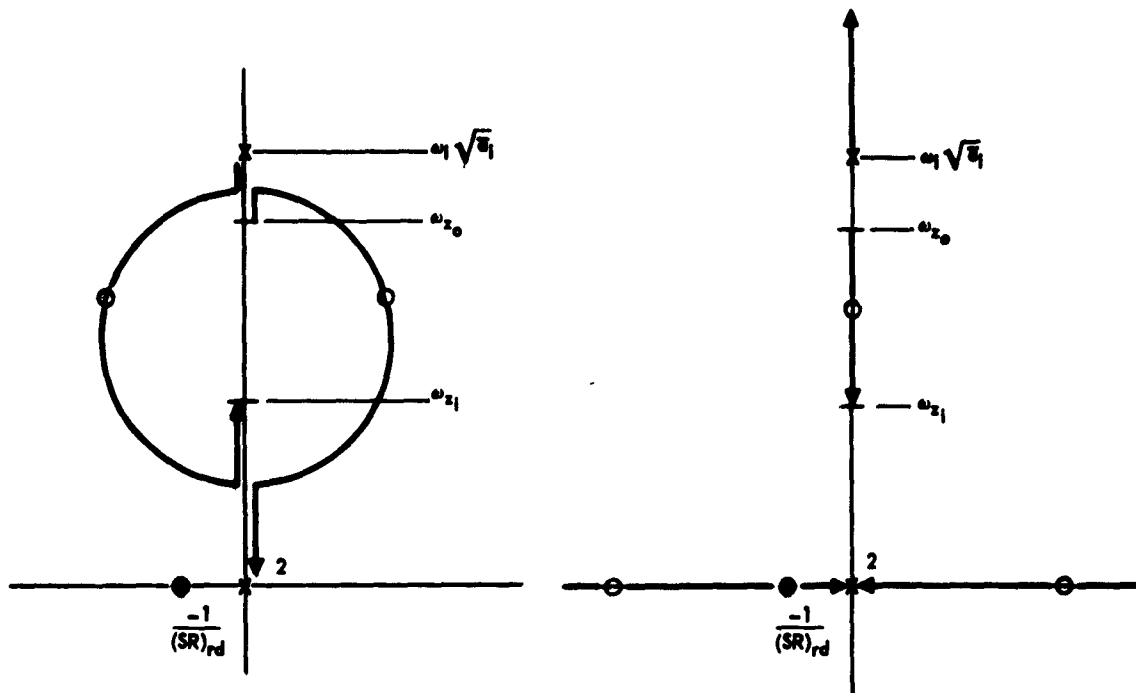
d. Case 4 ( $\lambda_{G_1}/\phi_{g_1} > 0, \omega_1 \sqrt{\alpha_1}/\omega_{z_1} > 1$ )

Fig. 5(a-d). Examples illustrating the different pole-zero configurations of  $(RF)_b[\delta; \delta_c^*]$  (including one bending mode, and assuming  $\lambda_{G_1} = \lambda_{r_{g_1}} = \lambda_{i_{g_1}}$ ).



  
 INCREASING MAGNITUDE OF "OPEN LOOP GAIN,"  $k_i$ , OF THE ROOT LOCUS OPERATION

e. Possible zero locations for Case 3 of Fig. 6(c).



f. A variation of Case 3 ( $\omega_1 \sqrt{\alpha_1} > \omega_{z_0}$ )

g. A variation of Case 4 ( $\omega_1 \sqrt{\alpha_1} < \omega_{z_0}$ )

Fig. 5 (e, f, g). Examples illustrating the different pole-zero configurations of  $(RF)_b [s; \delta_c^*]$ .  
 (including one bending mode, and assuming  $\lambda_{G_1} = \lambda_{r\theta_1} = \lambda_{l\theta_1}$ ).

Table 1. Tabulation of the phase (or range of phase) of  $(RF)_b[\delta; \delta_c^*] / [1 + p(SR)_{rd}]$  evaluated at its singularities in the upper half of the complex plane. This is for the cases of  $(RF)_b[\delta; \delta_c^*]$  illustrated in Fig. 5 a-g.

Case	Conditions		Phase at the singularities of $(RF)_b[\delta; \delta_c^*] / [1 + p(SR)_{rd}]$ (in degrees of lag)			
	Relative Value of $\omega_1 \sqrt{a_1} / \omega_{z_1}$	Relative Value of $\lambda_{G_1} / \phi_{z_1}$	Rigid Body Poles	Poles of the $i$ th Bending Mode	Higher Frequency or RHP Zeros, or Zeros on Real Axis	Lower Frequency or LHP Zeros
1	< 1	< 0	0°	90°	90°	90°
2	< 1	> 0	0°	270°	90° or 0° and 180°	270°
3	> 1	< 0	0°	270°	90°, or 180° to 0°, or 270°	270°, or 0° to -180°, or 90°
4	> 1	> 0	0°	90°	90° or 0° and 180°	90°

RHP = right hand half of the complex plane  
LHP = left hand half of the complex plane

Table 2. Tabulation of the possible locations of the zeros of  $(RF)_b[\delta; \delta_c^*] / [1 + p(SR)_{rd}]$  in the upper half of the complex plane for the cases illustrated in Fig. 5 a-g.

CASE	LOCATION OF THE ZEROS ASSOCIATED WITH THE $i$ th MODE	LOCATION OF THE "TAIL-WAGS-DOG" ZEROS OF THE BOOSTER
1	On the imaginary axis between $\omega_1 \sqrt{a_1}$ and 0	On the imaginary axis between $\omega_{z_0}$ and $\omega_{z_1}$
2	On the imaginary axis between $\omega_{z_1}$ and $\omega_1 \sqrt{a_1}$	On the imaginary axis between $\omega_{z_0}$ and $\omega_0$ or on the real axis
3	Both zeros are found on the imaginary axis between $\omega_1 \sqrt{a_1}$ and $\omega_{z_0}$ ; or One zero occurs in the RHP and the other occurs in the LHP between the greater of $\omega_1 \sqrt{a_1}$ and $\omega_{z_0}$ , and 0; or Both zeros are found on the imaginary axis between $\omega_{z_1}$ and 0.	
4	On the imaginary axis between $\omega_1 \sqrt{a_1}$ and $\omega_{z_1}$	On the imaginary axis between $\omega_{z_0}$ and $\omega_0$ or on the real axis

RHP = right hand half of the complex plane  
LHP = left hand half of the complex plane

control system may be troublesome and those areas where design will be straight forward.

#### RELATION OF CONTROL SYSTEM ANALYSIS TO CONTROL SYSTEM DESIGN

The design process consists of matching the sign of  $\lambda_{rg_i} / \phi_{g_i}$  with a compensation which provides the proper phasing of the  $i^{\text{th}}$  mode feedback signal to produce a maximum of artificial phase stabilization for the  $i^{\text{th}}$  mode. Alternatively, the compensation may provide sufficient attenuation of the  $i^{\text{th}}$  mode feedback signal to insure stability of the mode regardless of the sign of the  $i^{\text{th}}$  bending mode pickup and the phase shifts due to the remainder of the system. This process is carried out for all the modes which are included in the analysis. A combination of the above compensation methods may be employed for stabilization of a mode with success; however, such a system requires extensive study to insure the preservation of specified stability margins of both phase and gain.

As previously shown the locations of the zeros of the open loop booster relating function are influenced by the relative values of  $\omega_i \sqrt{a_i} / \omega_{z_i}$  to unity and  $\lambda_{rg_i} / \phi_{g_i}$  to zero. The effect of some of these possible locations on the system dynamics and general design procedure is illustrated by a simple example considering the rigid booster and one bending mode. The nozzle and actuator dynamics are represented as a single first order lag; this assumes that the second order dynamics associated with the nozzle-actuator linkage are negligible. The rate and rate integrating gyros are located at the same station along the booster body. ( $\lambda_{G_1} = \lambda_{rg_1} = \lambda_{ig_1}$ ) The performance functions of  $c_1$  and  $c_3$  compensation elements are equal to unity. The dynamics of the forward path compensation, (PF)  $c_2$ , are used to phase compensate the system used in this example.

The performance function for the closed loop control system can be developed from Figs. 1 and 3. This is given below.

$$(PF)_{bcs}[\theta_c; \delta] = \frac{S_{oc} \{ (PF)_n[\delta_c; \delta] (PF)_{c_2} \}}{1 + S_{oc} \{ (PF)_n[\delta_c; \delta] (RF)_b[\delta; \delta_c'] (PF)_{c_2} \}}$$

The characteristic roots of the booster flight control system are the poles of  $(PF)_{bcs}[\theta_c; \delta]$ . These may be determined from the above equation using root locus techniques.

If the departure and arrival angles for this root locus are calculated for a case without compensation,\*  $(PF)_{c_2} = 1$ , the approximate phase angle required of  $(PF)_{c_2}$  at the bending frequency to maximize the negative real coordinate of the closed loop bending poles becomes apparent. A suitable type of compensation may then be chosen to provide the needed phase shift at the bending frequency without causing the rigid body response to change by any substantial amount.

Figure 6 presents sketches of the root locus for three cases of the possible locations of the zeros of  $(RF)_b[\delta; \delta_c']$  with and without second order low pass compensation to achieve phase shift at the bending frequency. It is obvious that Figs. 6(a), (d), and (e) represent cases of correctly compensated systems, and that (b), (c) and (f) represent cases of incorrectly compensated systems.

It is quite possible for the booster flight control system to change from one of the situations illustrated in Fig. 6 to another during the flight of a typical booster. For instance:

1. If the bending mode resonant frequency becomes greater than the "tail-wags-dog" frequency of the mode during the booster

---

\* see Fig. 6(a), (c), and (e)

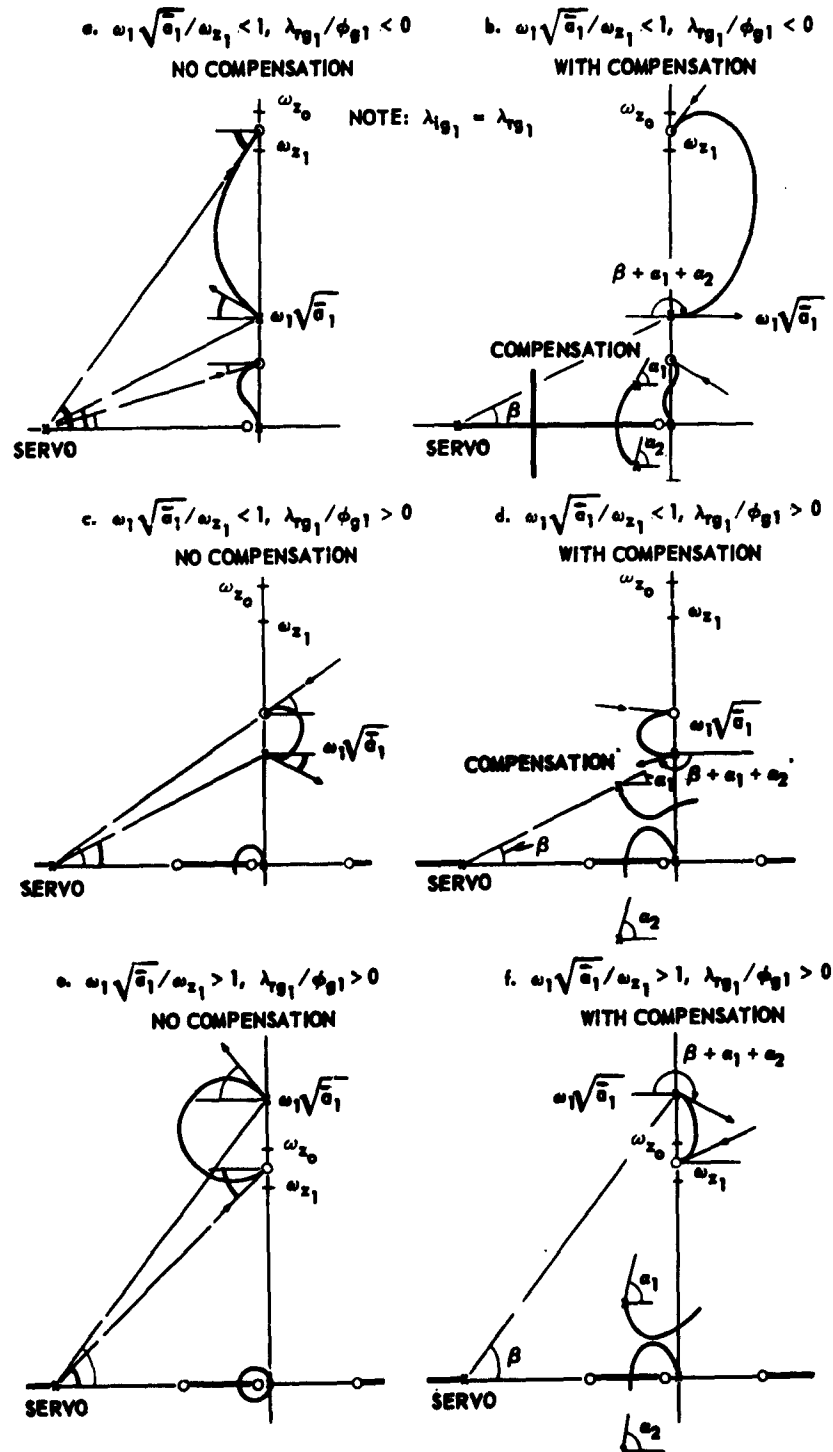


Fig. 6(a-f). Root locus diagrams for booster flight control systems including: booster and one bending mode (several types) and control system with and without compensation  $(PF)_{bc}[\theta_c; \delta] \cdot (RF)_b[\delta; \delta_c^*]$  versus  $S_{oc}$  for a fixed value of  $(SR)_{rd}$ .

flight\* ( $\omega_1 \sqrt{\bar{a}_1} / \omega_{z_1} < 1$  changes to  $\omega_1 \sqrt{\bar{a}_1} / \omega_{z_1} > 1$ ) the system changes from the situation illustrated in Fig. 6(d) to that in Fig. 6(f).

2. If the rate gyro is located such that the mode slope sensed by the gyro changes sign during the booster flight\*\* ( $\lambda_{r g_1} / \phi_{g_1} < 0$  changes to  $\lambda_{r g_1} / \phi_{g_1} > 0$ ) the system changes from the situation illustrated in Fig. 6(a) to that in Fig. 6(c).

If such a change of booster parameters does occur, it is necessary to make corresponding changes in the flight control system parameters to preserve the desired performance.

A case considering additional bending modes may be handled in a manner similar to the example. However, this would impose additional constraints upon the choice of  $(PF)_{c_2}$ . In the case of modes being phase stabilized, the approximate phase of  $(PF)_{c_2}$  at the bending mode resonant frequencies would be specified by the choices of the signs for  $\lambda_{G_1} / \phi_{g_1}$  and by the requirement that the negative real coordinate for each of the closed loop bending poles be increased. In the case of modes being amplitude stabilized, the maximum allowable gain of  $(PF)_{c_2}$  at the bending mode resonant frequencies would be specified.

### SUMMARY

This paper has advanced a simplified concept of analysis for a flexible booster flight control system. The main concern has been the development of a simplified, factored, open loop relating function for the booster control system. This provides the key to the evaluation of system performance. It was shown in the closing section that once this relating function has been evaluated, the closed loop system performance can be assessed using straightforward and familiar techniques.

---

\*see first footnote on page 14

\*\*Changes in the sign of a mode slope sensed by a gyro occur due to the wide variation of the booster mass distribution during the flight profile. This is very likely to occur when an attempt is made to place a gyro near an antinode of a particular mode.

This analysis is unique in that it enables this very complicated dynamics problem to be discussed and interpreted intelligently in qualitative terms. An engineer thoroughly familiar with this method can, on a moments notice, be prepared to discuss the control problems involved in the preliminary design of a particular booster. The knowledge required for discussion involves only well known quantities such as thrust, moment of inertia, nozzle mass, rough estimates of the bending mode frequencies, mode shapes, and slopes for the particular booster.

There are a host of points concerning the booster flight control system problem which are not suitable for presentation here with the fundamental principles, but which may be adequately treated by the methods of this analysis. Among these are the effects of: elements of the  $c_1$  compensation unit in the rate damping loop which do not appear in the orientation control loop, elements of the  $c_3$  compensation unit in the orientation control loop which do not appear in the rate damping loop, aerodynamics, propellant sloshing modes, and the couplings of bending and sloshing modes with the actuator-nozzle motion.

**APPENDIX A**  
**APPROXIMATE LINEARIZED EQUATIONS OF MOTION**  
**IN A SINGLE PLANE FOR A FLEXIBLE BOOSTER**

The perturbation equations of motion of the booster in a single plane used as the basis of this study are essentially those developed in Reference 2. These have been restated in a slightly different coordinate system and notation (standard aircraft body axis coordinate system) in Equation Summary A-1. The coordinate system definition and the definition of important system physical constants are shown in Fig. A-1.

These equations can be further simplified while still retaining the essential dynamic features resulting from the structural degrees of freedom of the physical system.

The simplifying assumptions are as follows:

1. Aerodynamics are neglected.
2. Cross couplings among the bending modes and couplings of the bending modes with the rigid body modes due to engine thrust are negligible.
3. Couplings of the bending modes with the nozzle dynamics are neglected.

The advantages of using these assumptions for simplifying the equations of motion are as follows:

1. The rigid body mode and the individual bending modes of the booster are decoupled from one another in the approximate equations of motion. This isolates the important bending effects.
2. The relations between  $\delta$  and the  $q$ ,  $\alpha$ ,  $a_z$ , and  $q_i$  variables (or their time derivatives) become simple second order differential equations. The approximate response of any of these variables may be examined by cascading a simple relating function with that describing  $\delta$  for the closed loop

booster flight control system. The low frequency response of these variables is well approximated only when the dynamic pressure is low. The high frequency response (the major concern of this report) is unaffected by neglecting the aerodynamics.

3. When the nozzle dynamics are considered separately from the booster body motion, the effects of inertial reaction torques which couple the rigid body and bending modes with the nozzle dynamics may be described by a feedback of each of these simple, second order, uncoupled modes around the second order nozzle dynamics.

The introduction of these assumptions after elimination of the intermediate variables  $v$ ,  $w$ ,  $u_g$ , and  $\psi_g$  by substitution reduces the equations of motion to those of Equation Summary A-2.

**EQUATION SUMMARY A-1  
FLEXIBLE BOOSTER EQUATIONS OF MOTION**

Normal force equation

$$m a_z = [C_{n_\alpha} qS] \alpha - [m g \cos \beta] \theta + [(C_{n_\alpha} + C_D) qS] w - [T] \psi_g - [T] \delta \quad (A1-1)$$

Components of normal acceleration

$$a_z = [Vp + a_x] \alpha - [Vp] \theta \quad (A1-2)$$

External moment equation

$$[I p^2] \theta = -[C_{n_\alpha} \ell_p qS] \alpha + [C_D qS] v - [C_{n_\alpha} \ell_p qS] w + [T] u_g - [T \ell_g] \psi_g - [T \ell_g] \delta \quad (A1-3)$$

Deflection of center line due to nozzle deflection

$$[m] v = -[\ell_n m_n] \delta \quad (A1-4)$$

Rotation of center line due to nozzle deflection

$$[I] w = -[I_E] \delta \quad (A1-5)$$

Deflection at the engine gimbal point

$$u_g = [l] v + [\ell_g] w + [\phi_{g_1}] q_1 + [\phi_{g_2}] q_2 + \dots + [\phi_{g_i}] q_i \quad (A1-6)$$

Slope at the engine gimbal point

$$\psi_g = [l] w - [\lambda_{g_1}] q_1 - [\lambda_{g_2}] q_2 - \dots - [\lambda_{g_i}] q_i \quad (A1-7)$$

$i^{\text{th}}$  bending mode generalized coordinate

$$[m p^2 + 2m \zeta_i \omega_i p + m \omega_i^2] q_i = -[(T + C_D qS) \lambda_{g_i}] v - [T \phi_{g_i}] \psi_g - [m_n \ell_i p^2 + T \phi_{g_i}] \delta \quad (A1-8)$$

Nozzle moment equation

$$[I_n p^2 + 2 I_n \zeta_n \omega_n p + I_n \omega_n^2] \delta = [\omega_n^2 I_n] \delta_a - [\ell_n m_n] a_z - [I_E p^2 + \ell_n m_n g \cos \beta] \theta + [T + C_D qS] v - [\ell_n m_n p^2] u_g - [I_n p^2 + (m_n \ell_n / m) (T + C_D qS)] \psi_g \quad (A1-9)$$

Motion sensed by the ( ) gyro

$$\begin{aligned}\dot{\theta}(\ ) &= [\rho]\theta + [\rho]w - \sum_i [\rho \lambda(\ )_i] q_i \\ &= [\rho]\bar{\theta} - \sum_i [\rho \lambda(\ )_i] q_i\end{aligned}\tag{A1-10}$$

---

**NOTES:** *These equations are modified from those of Ref. 2 by a change in the definition of the coordinate system and a change in the number of nozzles swiveled in a single plane. The effect of a distributed aerodynamic normal force on the bending has been neglected. Fuel sloshing effects have been neglected.*

*In general,  $C_{n_\alpha}$  and  $C_D$  are negative.*

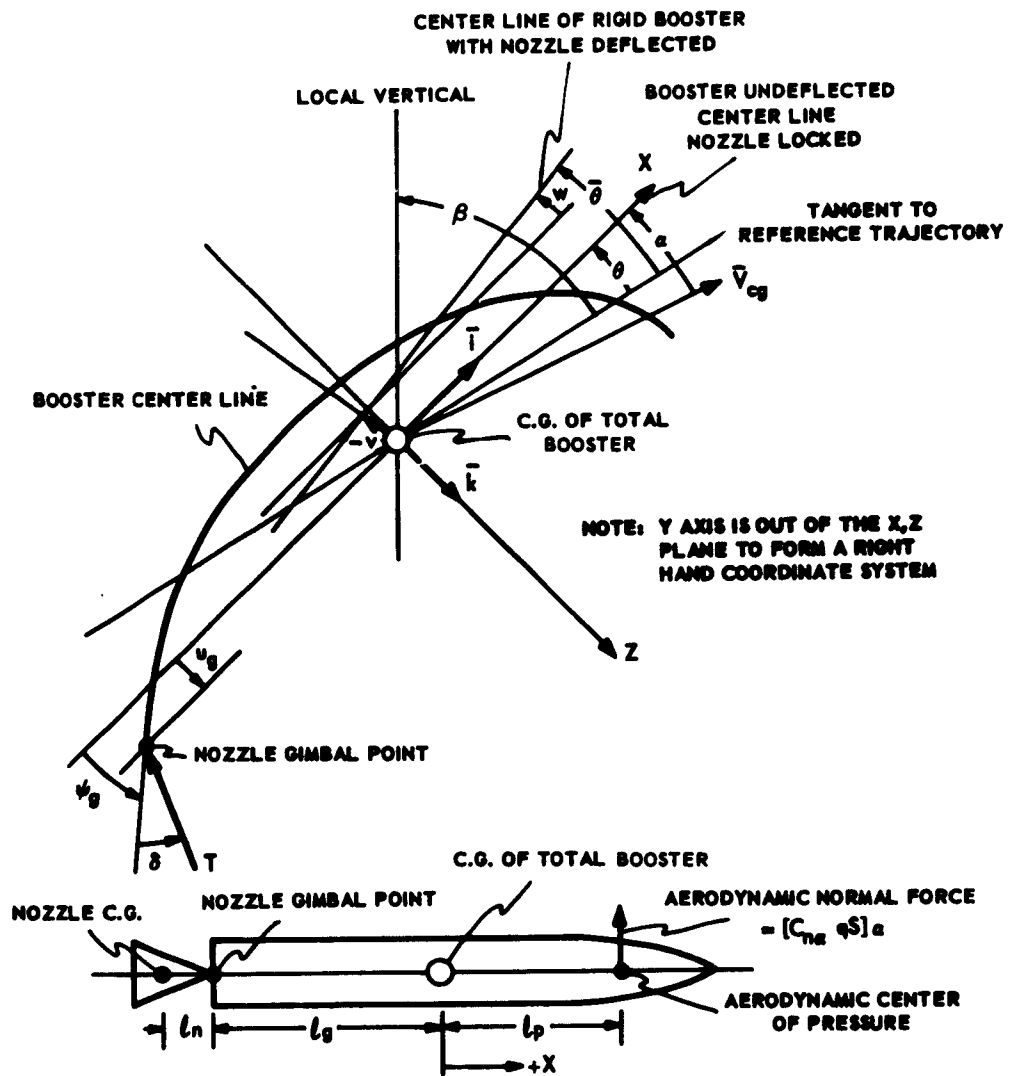


Fig. A-1. Coordinate system for analysis of the flexible booster.

**EQUATION SUMMARY A-2**  
**SIMPLIFIED FLEXIBLE BOOSTER EQUATIONS OF MOTION**

**Normal force equation**

$$[m]a_z = -[mg \cos \beta] \theta - \left[ T \left( 1 - \frac{I_E}{I} \right) \right] \delta \quad (A2-1)$$

**Components of normal acceleration**

$$a_z = [Vp + a_x] \alpha - [Vp] \theta \quad (A2-2)$$

**External moment equation**

$$[I p^2] \theta = - \left[ T l_g \left( 1 + \frac{m_n l_n}{m l_g} \right) \right] \delta \quad (A2-3)$$

**Generalized coordinate of the  $i^{\text{th}}$  bending mode**

$$\begin{aligned} & \left[ m (p^2 + 2 \zeta_i \omega_i p + \omega_i^2) - T \phi_{g_i} \lambda_{g_i} \right] q_i = \\ & \left[ T l_g \lambda_{g_i} \frac{m_n l_n}{m l_g} - T \phi_{g_i} \left( 1 - \frac{I_E}{I} \right) - p^2 m_n l_i \right] \delta \end{aligned} \quad (A2-4)$$

**Nozzle moment equation**

$$\begin{aligned} & \left[ I_n (p^2 + 2 \zeta_n \omega_n p + \omega_n^2) - \frac{T l_g}{I} \left( 1 + \frac{m_n l_n}{m l_g} \right) I_E + \right. \\ & \left. - p^2 \left( \frac{m_n^2 l_n^2}{m} + \frac{I_E^2}{I} \right) \right] \delta = [I_n \omega_n^2] \delta_a \end{aligned} \quad (A2-5)$$

**Motion sensed by the ( ) gyro**

$$\begin{aligned} \dot{\theta}_{( )} &= \dot{\theta} - \left[ p \frac{I_E}{I} \right] \delta - \sum_i [p \lambda_{( )}_i] q_i \\ &= \dot{\theta} - \sum_i [p \lambda_{( )}_i] q_i \end{aligned} \quad (A2-6)$$

APPENDIX B  
OBTAINING THE FLEXIBLE BOOSTER RELATING  
FUNCTION WHICH INCLUDES COMPENSATION

The method used in Equation Summary 1 to develop the relating function  $(RF)_{b[\delta; \delta_c'']}$  has been extended to include different compensation elements in each of the gyro signal paths. The results are summarized in Equation Summary B-1.

The compensation used in each gyro path is required to be in factored form and the numerator and denominator orders must be equal. If the number of finite poles should exceed the number of finite zeros in the actual compensation being investigated, additional zeros must be carried at infinity to equalize the numerator and denominator orders. The rate path compensation is given as  $(PF)_{c_1} = N_1(p)/D_1(p)$ , where the order of  $N_1$  and  $D_1$  is  $p^u$ ; and the rate integrating path compensation is given as  $(PF)_{c_3} = N_3(p)/D_3(p)$ , where the order of  $N_3$  and  $D_3$  is  $p^v$ . The number of zeros associated with  $(RF)_{b[\delta; \delta_c'']}$  when written as a rational polynomial is  $(2n + u + v + 1 + 2)$ . Some of these zeros may occur at infinity as previously mentioned. The  $(2n + u + v)$  zeros result from placing the polynomials over a common denominator; two "tail-wags-dog" zeros from the inertial reactions of the gimbaled nozzle; and one zero from the rate gyro "differentiation". In addition it is required that  $N_1(0)/D_1(0) = N_3(0)/D_3(0) = 1$ .

This additional generalization increases the complexity of the expression for  $(RF)_{b[\delta; \delta_c'']}$  quite substantially because of factorizations of  $(N_3 D_1 + [\text{const.}] p N_1 D_3)$  which must be performed for each mode included in the analysis. (See Eqs. B1-1, B1-2 and the associated auxiliary equations of Equation Summary B-1.)

The equations for  $(RF)_{b[\delta; \delta_c^*]}$  with  $(PF)_{c_1} \neq 1 \neq (PF)_{c_3}$  are presented below without derivation. The method of derivation is essentially similar to that of Equation Summary 1.

The relating function including the 1st bending mode in parallel with the rigid body is

$$(RF)_{b[\delta; \delta_c^*]} = \frac{S_b[\delta; \theta]}{p^2 D_1 D_3 \left(1 + \frac{2\zeta_1}{\bar{\alpha}_1 \omega_1} p + \frac{p^2}{\bar{\alpha}_1 \omega_1^2}\right)} \left[ \left\{ \frac{K_1 \frac{B_1}{A_1}}{1 + K_1 \frac{B_1}{A_1}} \right\} \frac{1}{K_1 \frac{B_1}{A_1}} \right]^{-1} \quad (B1-1)$$

where

$$A_1(p) = (N_3 D_1 + p (SR)_{rd} N_1 D_3) \left(1 + \frac{2\zeta_1}{\bar{\alpha}_1 \omega_1} p + \frac{p^2}{\bar{\alpha}_1 \omega_1^2}\right) \left(1 + \frac{p^2}{\omega_{z_0}^2}\right) \quad (B1-1a)$$

$$B_1(p) = p^2 \left(N_3 D_1 + p (SR)_{rd} \frac{\lambda_{rg1}}{\lambda_{ig1}} N_1 D_3\right) \left(1 + \frac{p^2}{\omega_{z_1}^2}\right) \quad (B1-1b)$$

$$K_1 = \frac{-\lambda_{ig1} S_b[\delta; \theta]}{S_b[\delta; \theta]} \quad (B1-1c)$$

Equation Summary B-1 (Page 1 of 2)

Equations for the Flexible Booster Relating  
Function Which Includes Compensation

The relating function for  $n$  bending modes can be obtained by performing the following operations on the relating function which includes  $(n-1)$  bending modes ( $n = 2, 3, \dots$ ). The effects of the  $j^{\text{th}}$  bending mode will be added.

$$(RF)_{b[\delta; \delta_c^*]} = \frac{S_b[\delta; \tilde{\theta}]}{p^2 D_1 D_3 \prod_i^n \left(1 + \frac{2\zeta_i}{\bar{a}_i \omega_i} p + \frac{p^2}{\bar{a}_i \omega_i^2}\right)} \left[ \left\{ \frac{K_j \frac{B_j}{A_j}}{1 + K_j \frac{B_j}{A_j}} \right\} \frac{1}{K_j \frac{B_j}{A_j}} \right]^{-1} \quad (B1-2)$$

where

$$A_j(p) = \left\{ \text{the } (2n + u + v + 1) \text{ zeros of } (RF)_{b[\delta; \delta_c^*]} \text{ for } (n-1) \text{ bending modes} \right\} \left(1 + \frac{2\zeta_j}{\bar{a}_j \omega_j} p + \frac{p^2}{\bar{a}_j \omega_j^2}\right) \quad (B1-2a)$$

$$B_j(p) = p^2 \left( N_3 D_1 + p (SR)_{rd} \frac{\lambda_{rgj}}{\lambda_{igj}} N_1 D_3 \right) \left(1 + \frac{p^2}{\omega_{zj}^2}\right)^{n-1} \prod_i \left(1 + \frac{2\zeta_i}{\bar{a}_i \omega_i} p + \frac{p^2}{\bar{a}_i \omega_i^2}\right) \quad (B1-2b)$$

$$K_j = \frac{-\lambda_{igj} S_b[\delta; q_j]}{S_b[\delta; \tilde{\theta}]} \quad (B1-2c)$$

The  $2n + u + v + 1$  zeros of Eq. (B1-2a) must be expressed in the form  $\left(1 + \frac{2\zeta}{\omega} p + \frac{p^2}{\omega^2}\right)$  or  $(1 + \tau p)$ .

Equation Summary B-1 (Page 2 of 2)

Equations for the Flexible Booster Relating  
Function Which Includes Compensation

GLOSSARY  
SYMBOLS

- $C_D$  = aerodynamic drag coefficient,  $C_D = \frac{D}{qS}$
- $C_{N_\alpha}$  = aerodynamic normal force coefficient,  $C_{N_\alpha} = \frac{\partial N / \partial \alpha}{qS}$
- $D$  = aerodynamic drag force
- $I$  = total moment of inertia of booster about the center of mass
- $I_E = I_n + m_n l_n l_g$
- $I_n$  = moment of inertia of nozzle about gimbal point
- $K_i$  = non-dimensional "open loop gain" used in the root locus factorization of the numerator of  $(RF)_b[\delta; \delta_c^*]$  when the effects of the  $i$ th bending mode are being added.
- $N$  = aerodynamic normal force
- $(PF)_n[q_{in}; q_{out}]$  = performance function of component  $n$ , relating the measurable output,  $q_{out}$ , to the measurable input,  $q_{in}$
- $(RF)_n[q_{in}; q_{out}]$  = relating function describing the mathematical relationship between the output,  $q_{out}$ , and input,  $q_{in}$ , of component  $n$
- $S$  = reference area
- $S_{oc}[\dot{\theta}_{ig}; \delta_\alpha]$  = sensitivity of the orientation control loop ( $S_{oc}$ )
- $S_{rd}[\dot{\theta}_{rg}; \delta_\alpha]$  = sensitivity of the rate damping loop ( $S_{rd}$ )
- $(SR)_{rd}$  = rate damping sensitivity ratio  $(SR)_{rd} = S_{rd}/S_{oc}$
- $S_n[q_{in}; q_{out}]$  = static sensitivity of the performance function or relating function of component  $n$  relating the output,  $q_{out}$ , to the input,  $q_{in}$
- $T$  = thrust
- $V$  = booster velocity
- $\bar{a}_i$  = modification factor for natural bending characteristics of the  $i$ th mode when the rocket engine is thrusting  $\bar{a}_i = 1 - \frac{T \phi_{\theta_i} \lambda_{\theta_i}}{m \omega_i^2}$

- $a_x, y, \text{ or } z$  = acceleration of booster center of mass in the positive x, y, or z direction
- $g$  = acceleration of gravity
- $k_i$  = dimensional form of  $K_i$ ; the form of the open loop gain actually used in performing root locus factorizations.
- $$l_i = l_n \phi_{g_i} - \frac{I_n}{m_n} \lambda_{g_i}$$
- $l_g$  = distance between the booster center of mass and the nozzle gimbal point
- $l_n$  = distance between the center of mass of the nozzle and the gimbal point
- $l_p$  = distance between center of pressure and the center of mass (positive for center of pressure forward of the center of mass)
- $m$  = total mass of booster
- $m_n$  = mass of the nozzle
- $p$  = Laplace operator; a complex number  $p = \sigma + j\omega$  ( $\sigma$  and  $\omega$  are real numbers,  $j = \sqrt{-1}$ )
- $q$  = dynamic pressure
- $q_i$  = generalized deflection coordinate of the  $i^{\text{th}}$  bending mode
- $t$  = time
- $u(\ )$  = deflection from the undeformed elastic axis at the station identified by the subscript
- $v$  = translation of the rigid body from the x axis in the z direction due to negative nozzle deflection ( $T = 0$ )
- $w$  = rotation of the rigid body centerline from x axis due to negative nozzle deflection ( $T = 0$ )
- $\alpha$  = angle of attack - angle from the velocity vector to the undeformed elastic axis
- $\beta$  = angle from the reference trajectory to the local vertical
- $\delta$  = nozzle deflection angle from the centerline of booster at the gimbal point to the centerline of the rocket nozzle
- $\delta_a$  = hydraulic actuator output in units of equivalent nozzle deflection
- $\delta_c$  = commanded nozzle deflection
- $\zeta(\ )$  = damping ratio or effective damping ratio of the mode indicated by the subscript
- $\theta$  = angle from the reference trajectory to the undeformed elastic axis
- $\bar{\theta}$  = angle from the reference trajectory to the rigid body centerline (nozzle deflected)

- $\theta_c$  = commanded angle from reference trajectory to undeflected booster centerline  
 $\dot{\theta}(\ )$  = angular velocity sensed by a gyro located at station indicated by subscript  
 $\lambda(\ )_i$  = normalized  $i^{\text{th}}$  bending mode slope amplitude at station identified by subscript  $\lambda(\ )_i = \frac{\partial \phi}{\partial X} i |(\ )$   
 $\phi(\ )_i$  = normalized  $i^{\text{th}}$  bending mode deflection amplitude at station identified by subscript  
 $\psi(\ )$  = slope of the booster centerline with respect to the undeformed elastic axis at the station indicated by the subscript  
 $\omega(\ )$  = undamped natural frequency or effective undamped natural frequency of the mode indicated by the subscript

- NOTES: (1) Station numbers are distances from a reference point on the undeflected center line. This reference is usually chosen forward of the nose and is positive in the opposite sense to the x axis.  
 (2) All angles are defined as positive for a small angle vector treatment in which the vector sense is positive.

#### SUBSCRIPTS

- $a$  = control system actuator or servo  
 $i$  =  $i^{\text{th}}$  bending mode ( $i = 1, 2, 3, \dots$ )  
 $ig$  = rate-integrating gyro  
 $b$  = booster  
 $bcs$  = booster flight control system including booster  
 $n$  = nozzle  
 $rg$  = rate gyro  
 $z_0, z_i$  = "tail-wags-dog" zero of rigid body or  $i^{\text{th}}$  bending mode

## REFERENCES

1. Kezer, A., Hofmann, L. G., "Model Reference Adaptive Control System Design and Analysis Techniques for Large Flexible Missile Flight Control Systems, "Instrumentation Laboratory, Massachusetts Institute of Technology (being prepared for publication).
2. Trembath, N. W., "Dynamic Equations for Minuteman Missile,"(Space Technology Laboratories, California, July 20, 1959).
3. Lanzer, L. F., "Simplified Bending Analysis for Gyros at Different Stations, "Report GM42.4-39, (Space Technology Laboratories, California, January 22, 1958).
4. Kezer, A., "A Preliminary Investigation of Problems Arising in the Control of Large Flexible Missiles, "Report E-927, Instrumentation Laboratory, Massachusetts Institute of Technology, June 1960.